Date of publication xxxx 00, 0000, date of current version xxxx 00, 0000.

Digital Object Identifier 10.1109/ACCESS.2023.DOI

GearFaultNet: Novel Network for Automatic and Early Detection of Gearbox Faults

PROMA DUTTA[1♠], KANCHON KANTI PODDER[1♠], MD. SHAHEENUR ISLAM SUMON[2], MUHAMMAD E. H. CHOWDHURY[2*], AMITH KHANDAKAR[2], NASSER AL-EMADI[2], MOAJJEM HOSSAIN CHOWDHURY[3], M. MURUGAPPAN[4,5], MOHAMED ARSELENE AYARI[6], SAKIB MAHMUD[2], S. M. MUYEEN[2]

[1]Department of Electrical and Computer Engineering, Kennesaw State University, Marietta, GA 30060, USA
[2]Department of Electrical Engineering, Qatar University, Doha 2713, Qatar
[3]Department of Electrical, Electronic and System Engineering, Universiti Kebangsaan Malaysia, Bangi 43600, Malaysia
[4]Intelligent Signal Processing (ISP) Research Lab, Department of Electronics and Communication Engineering, Kuwait College of Science and Technology, Block 4, Doha 13133, Kuwait
[5]Department of Electronics and Communication Engineering, School of Engineering, Vels Institute of Sciences, Technology, and Advanced Studies, Chennai, Tamil Nadu, India
[6]College of Engineering, Qatar University, Doha 2713, Qatar

♠Co-first Authors
*Corresponding author: Muhammad E. H. Chowdhury (mchowdhury@qu.edu.qa)

ABSTRACT Electrical and mechanical equipment with rotating parts often face the challenge of early breakdown due to defects in the gears or rolling bearings. Automated industrial systems can be significantly impeded by this type of fault in revolving components because of manual fault detection and the additional time required for repairing and replacing them. This research presents GearFaultNet, a novel, lightweight 1D Convolutional Neural Network (CNN)-based network, designed to detect gearbox faults. GearFaultNet can be an effective measure for real-time detection of sudden shutdowns and can alleviate downtime and system losses in the industrial aspect. The proposed framework involves the integration of four-channel vibration data from different loading conditions, which are preprocessed in the temporal domain and fed to GearFaultNet to classify the gearbox's condition as either Healthy or Broken. The developed lightweight deep learning network has achieved higher accuracy than those proposed in existing literature. The overall accuracy achieved by this framework is 94.04%. This shallow network can also be applied to estimate other mechanical faults in different machinery.

INDEX TERMS GearFaultNet, Fault Detection, Gearbox, 1D-CNN, Deep Learning

I. INTRODUCTION

The power system always requires condition monitoring to maintain robust and secure operation and ensure a safe supply to users. Condition monitoring is essential for preventing unplanned outages and preserving the reliability and safety of the electrical grid by detecting potential problems with equipment before they occur. In power systems, various approaches are employed for condition monitoring, such as monitoring electrical parameters like frequency, current, or voltage [1], vibration and oscillation analysis [2]-[5], analysis of oil or lubricant quality, insulation discharge monitoring, and temperature fluctuation analysis through Infrared radiation (IR) or thermal cameras [6], among others. A power system comprises generation, transmission, distribution, substations, and loads. Each sector requires a condition monitoring system with various critical monitoring applications to avoid system interruption and energy loss [7]. Switch-gear circuit breakers protect electrical systems against overload and short circuits. This is accomplished by regularly checking contact wear, braking speed, and timing [7]. Transformers are monitored for oil level, temperature, insulation resistance, and partial discharge. Power cables also have a similar status monitoring system, excluding oil level, to prevent system failure. Generators and motors are inspected using parameters such as temperature, voltage, current, frequency, revolutions per minute (RPM), vibration, and more [7].

Gearboxes are utilized in rotating instruments such as generators, wind turbines, hydro turbines, pump turbines, and marine current turbines (MCT) to mechanically transmit power at the required torque or speed. The operational range of variable-speed wind generators (VSWG) exceeds that of other types of wind turbines (WT) because they can adjust their rotating speed to match the wind's velocity [8]. Various types of wind generators can generate power at different speeds, including the doubly-fed induction generator (DFIG) [8], the variable speed drive (VSD), and others. The two primary types of issues that may arise with a WT generator are electrical and mechanical. Electrical problems include open circuits, voltage fluctuations, and damaged stator and rotor insulation [7]. Common mechanical problems comprise insufficient lubrication, a bent shaft, a fractured rotor bar, an irregular air gap, and a failed bearing [9]. Any problems with these components can result in unexpected and unscheduled downtime, costly maintenance, production losses, and delays in power delivery.

In 2014, there were more power outages than ever before, affecting 14.2 million people [10]. Identifying and predicting these defects early in the operation and maintenance process, as well as improving power output, are essential for preventing power outages and catastrophic failures. According to recent studies, gearbox failure results in more downtime than any other component. On average, 256 hours are spent maintaining gearboxes in wind turbines [11]. Failures in these turbines are caused by the gearbox in 59.1% of cases, by bearings in 76.1%, and by gears in 17.1% [11]. With various machine learning, deep learning models, and sophisticated spectrum analysis, artificial intelligence (AI) has become essential in rotating equipment for fault detection or estimating the "Remaining Lifetime" and replacements of various components. The growing prominence of deep learning in the field of signal processing is becoming increasingly evident [12]-[14]. Deep learning models have also proven their effectiveness in defect diagnosis using signals from gearboxes [15] and rolling bearings [16], which are detailed in the next section. Innovative, lightweight models are necessary for real-time usage in industrial sectors to detect faults in rotating equipment. Complex models or laborious preprocessing techniques could prolong fault prediction time, making them unsuitable for real-time applications. Thus, the contributions of this research can be highlighted as follows:

- The proposed framework offers a unique and efficient approach to gearbox fault detection in rotating equipment, providing a lightweight solution for real-time applications. It showcases the effectiveness of deep learning models in identifying and predicting defects, leading to improved operational efficiency and reduced downtime.
- The proposed framework facilitates efficient means for prompt detection of sudden shutdowns, reducing downtime and system losses in industrial environments. It also enables the timely detection of faults in rotating equipment, ensuring prompt maintenance and averting significant machinery failures.
- The novel *GearFaultNet* attains an overall accuracy of 94.06%, surpassing previous literature on gearbox fault detection. It also exhibits elevated precision, specificity, and recall, particularly in identifying faulty signals.
- The proposed approach holds promise for being utilized in fault estimation across a range of mechanical devices beyond gearboxes.

The rest of the paper is organized as follows: Section II explores previous research on gearbox fault detection and various methodologies employed. Section III outlines the methods and materials employed in this study. Section IV presents the results and discusses them using suitable evaluation metrics. Lastly, in Section V, conclusions are drawn, and future work is outlined.

II. LITERATURE REVIEW

In this section, we delve into a comprehensive background research encompassing several pivotal aspects of this study. Initially, we explore different types of gear faults. Subsequently, we provide an in-depth discussion of pertinent studies conducted on gear fault detection employing various techniques throughout the years.

A. TYPES OF GEAR FAULT

Conventional rotating machinery systems, including rotary kilns, wind turbines, water turbines, and steam turbines, play a crucial role as strategic assets supporting major businesses [17], [18]. Monitoring their condition and predicting faults is imperative to maintain their ongoing efficiency, safety, and reliability. Mechanical defects or faults in rotating machinery systems typically fall into three main categories: issues with the rotor body, problems with the rotor support bearing, and faults in the transmission gear [19]. The latter category encompasses conditions such as tooth breakage, spalling, missing teeth, surface wear, chipping of the tip, and tooth pitting. Fig. 1 illustrates various types of faulty gear conditions.

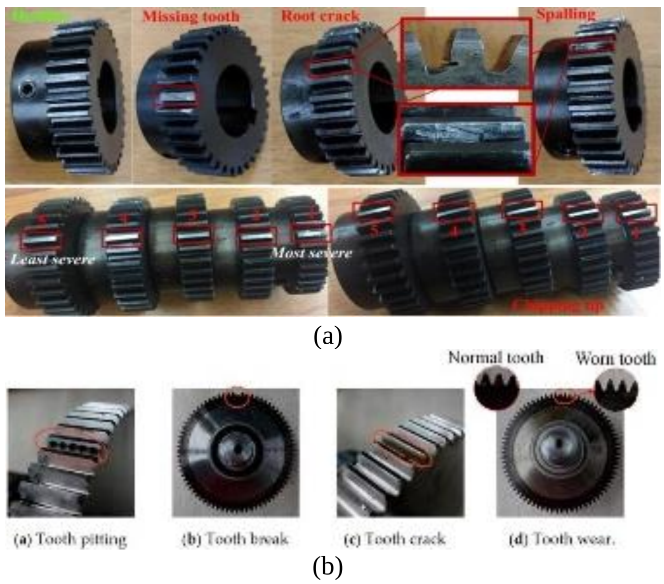

FIGURE 1. (a), (b) Different types of faults in the gearbox [20], [21].

B. GEAR FAULT DETECTION

The past decade has seen a proliferation of various machine-learning approaches in the monitoring and prediction of faults in rotating machinery. For fault detection, researchers employ diverse types of data, including vibration data [2]-[5], oil and gear bearing temperatures [22], vibration and current signals [1], and other combinations of time series data. In [23], the authors introduced a 1D deep neural transfer learning model to interpret torque measurements and predict the health status of gearboxes, achieving an accuracy of over 82% for different transfer tasks. Three deep neural network models, namely stacked autoencoders (SAE), deep belief networks (DBN), and deep Boltzmann machines (DBM), were investigated in [24]. Fault detection in rolling bearings was predicted through preprocessing methods in both the time and frequency domains, involving seven types of faults, and achieved an accuracy of over 99% for all three methods. The modified SAE model proposed in [25] outperformed the raw SAE by minimizing overfitting using the rectified linear unit (ReLU) activation function and the dropout technique.

This article has been accepted for publication in IEEE Access. This is the author's version which has not been fully edited and content may change prior to final publication. Citation information: DOI 10.1109/ACCESS.2024.3412274

On the other hand, a multiscale convolutional learning structure with an attention mechanism based on acoustic-based diagnosis demonstrated an 82.8% accuracy [26]. Fault feature vectors obtained through vibration signal decomposition using the Hilbert empirical wavelet transform (HEWT) were classified with a self-organizing map (SOM) model to detect faulty gears, as described in [27]. A deep random forest fusion approach was employed to integrate acoustical emission and vibrational data for the detection of 11 different condition patterns indicative of gearbox failures, resulting in a classification rate of 97.68 percent, as reported in [28]. Vibration signals were transformed into time-frequency spectral images using wavelet analysis integrated with a convolutional neural network (CNN) model [29], and the features from the images were then extracted to classify the faults. Specifically, for single-condition gearbox fault diagnosis, attentive kernel residual network (AKRNet) [30] achieved a high average recognition accuracy of 99.51% across various health states of the gearbox, including normal, worn teeth with five defect levels, pitting teeth, cracked teeth, and three bearing defects (inner race defect, ball defect, and cage defect).

Empirical mode decomposition (EMD), long short-term memory (LSTM), and particle swarm optimization (PSO) were combined in a novel deep neural network presented in the paper, achieving 97.44% accuracy [31]. Another hybrid attention-based method for fault diagnosis combined ResNet [32] and wavelet transform. A multi-scale fusion global sparse network, a specialized form of CNN for gearbox fault evaluation, is discussed in [4], achieving an overall accuracy of 98.45%. In [20], a novel method of gear fault diagnosis was proposed, combining a 1D denoising convolutional autoencoder (DCAE-1D) and a 1D-CNN with anti-noise improvement (AICNN-1D), resulting in improved accuracies of 89.12% and 92.24%, respectively. LSTM and its variant Bi-LSTM for gearbox fault estimation were compared in [33], achieving the best overall accuracy of 99.5%. Similarly, an application for diagnosing faults in a gearbox transmission chain using unsupervised deep belief networks is described in [34], where structural parameters are optimized using a genetic algorithm. This approach outperforms other machine learning techniques for classifying gearbox and bearing faults, achieving perfect accuracy for gearbox faults.

The literature referenced above [28]-[19] utilized various datasets, techniques, and categories for gear fault detection. However, the "Gear Box Fault Diagnosis Data Set" [35] was exclusively employed for binary class classification in this study, distinguishing between *Healthy* and *Broken* categories. While the authors in [3] achieved an accuracy of 87.5% using the "Sigmoid-PSO + Hybrid LSTM" and "ReLU-Cuckoo + Hybrid LSTM" techniques, the accuracy remained relatively low. Conversely, in [2], 100% accuracy was reported using "NLMS Error (Adaptive filter) + SVM", "EMD-IMF 1 + SVM", "Plain Method + SVM", and random sampling methods. However, the random sampling approach presents a risk of data leakage between training and test sets, rendering it ineffective for real-world applications [36]. Consequently, there exists a research gap regarding the "Gear Box Fault Diagnosis Data Set" for classifying fault signals by testing the model with various loading condition data to prevent data leakage between training and test sets. In this research, preprocessing was simplified, and a model with five layers of shallow 1D convolutional networks was developed, surpassing the findings of previous studies.

III. MATERIALS AND METHODS

In this section, we delve into the materials utilized and the methodologies adopted throughout this study. We commence by presenting a high-level overview of the deep learning-centered approach designed to detect gear faults from vibrational data. Following this, we examine the dataset, the steps involved in data preprocessing, the architecture of the proposed *GearFaultNet* model, the experimental setup, and the evaluation metrics devised for this research.

A. FRAMEWORK OVERVIEW

The proposed framework comprises two main sections: data preprocessing and 1D classification utilizing a deep-learning-based classifier. The vibrational sensor data utilized in this study for gear fault detection are one-dimensional (1D) signals necessitating thorough preprocessing before utilization. Following initial preprocessing steps, we create independent folds based on loading conditions to ensure the robustness of the study. Additionally, we augment the training sets in each fold by employing overlapping, as deep learning models exhibit a voracious appetite for data and often suffer from insufficient data abundance. Next, we perform the pivotal step of this research that involves classifying the raw sensor data into *Healthy* and *Broken* gear classes based on the input 1D signals, accomplished by the deep classifier. Finally, we assess the performance of our novel proposed *GearFaultNet* model using commonly utilized metrics detailed in upcoming sections. Ablation studies are also conducted wherein we compare *GearFaultNet's* performance against other state-of-the-art (SOTA) models. Furthermore, we contrast *GearFaultNet's* performance against existing studies in the current literature that have worked on the same dataset and attempted to classify the signal based on the presence of gear faults.

B. DATASET DESCRIPTION

This study utilizes a dataset generated from SpectraQuest's Gearbox Fault Diagnostics Simulator (GFDS), as outlined in [11]. The dataset is publicly accessible on the *data.world* repository [35]. The GFDS serves as a gearbox prognostics simulator, designed to replicate industrial gearboxes for research purposes. The simulator, depicted in Fig. 2, allows for the configuration of the gearbox with different gear ratios (ranging from 1 to 6) and various types of bearings, including rolling or sleeve bearings. Its development aims to offer researchers a broader range of gearbox configurations for investigating topics such as gearbox health monitoring, dynamics, and acoustic behavior, and vibration-based diagnostic and prognostic methods.

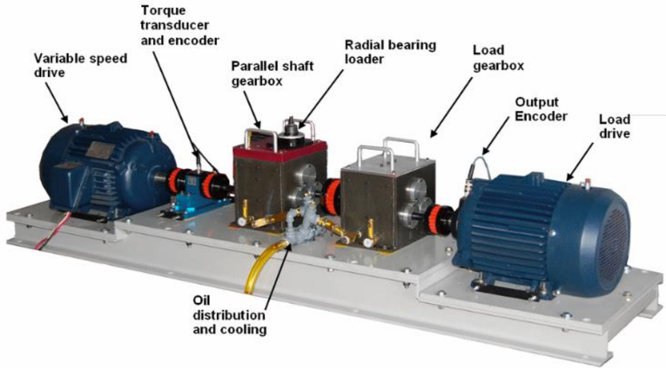

FIGURE 2. **SpectraQuest's Gearbox Prognostics Simulator (GPS) setup [37].**

The gearbox is engineered to support multiple sensor types. Diagnostics of rotating equipment and in-process monitoring necessitate drawing inferences about defects and process conditions based on sensor readings. These readings and process states often exhibit intricate and non-deterministic relationships. Enhanced performance typically requires the incorporation of multiple sensors. When employing multiple sensors, each sensor's information may offer distinct insights into the same machine's status. Accelerometers can be affixed to the bearing housing to measure vibrations in all three directions. In the dataset utilized for this study, four accelerometers were positioned on the gearbox body to capture vibration signals. The recorded data is categorized into two classes: *Healthy* and *Broken*. Both classes encompass 10 loading conditions, ranging from 0% to 90% in increments of 10%. Each condition is associated with four channels of data from four sensors, with a sampling frequency of 30 Hz.

C. DATA PREPARATION

In deep learning frameworks, temporal data must be divided into smaller, uniform segments [38]-[40]. Initially, we partitioned all data from the four channels into segments of 512 samples each. Deep learning models generally require a good number of high-quality samples to perform well in any task. In this case, the challenge of data limitations has been solved through augmentation. To enhance the training sets post-partitioning (i.e., fold creation), we employed a 50% overlapping technique, similar to studies in the domain of deep-learning-based 1D signal classification [43]-[45] or signal-to-signal reconstruction (segmentation) [46]-[49]. During overlapping, subsequent segments comprised half of the data samples from the preceding segments, and vice versa. For example, as shown in Fig. 3, the first segment encompasses the initial 512 samples of one sensor data for a loading condition of 10%, while the second segment begins from the 256th sample and extends to the 768th sample point, resulting in a total segment length of 512 samples.

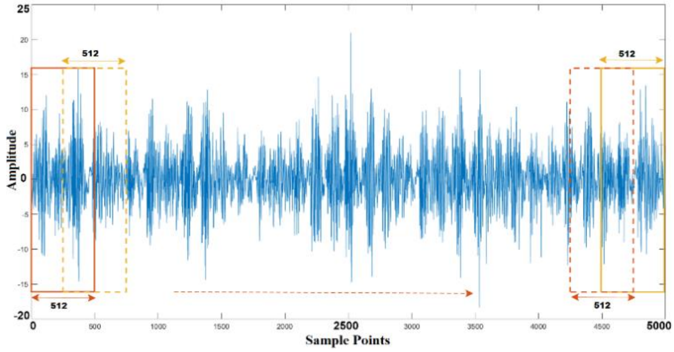

FIGURE 3. **A depiction of data augmentation through 50% overlapping**

Once the segments were generated, the data underwent normalization. Normalization is performed to ensure that all features are treated with equal importance. We utilized z-score normalization [46]-[48] separately for each of the four input channels. Z-score normalization involves transforming each value in a dataset so that the mean of all values becomes 0 and the standard deviation becomes 1. This process is also referred to as "Standard Scaling," as defined in (1).

$$\|\boldsymbol{x_i}\| = \frac{\boldsymbol{x_i} - \mu}{\sigma} \tag{1}$$

Here, $\boldsymbol{x_i}$ and $\|\boldsymbol{x_i}\|$ represent the ith raw and normalized samples, respectively, while μ and σ denote the sample mean and standard deviation, respectively, of all data within a specific channel. The vector quantities or arrays have been highlighted to distinguish them from the scalars. Following z-score normalization, we apply global min-max normalization (also known as range normalization), which is the most commonly used method for normalizing 1D signals in deep learning systems [40], [1], [45]-[50]. In this process, the minimum value of each segment is scaled to -0.2, and the maximum value is scaled to 0.2. Subsequently, intermediate values are then mapped within this range, as formulated in (2). Fig. 4 depicts a graphical representation of raw and preprocessed signals using a bell curve. Only two loading conditions (0% and 30%) are shown in Fig. 4, while a high-resolution version illustrating the normalized distribution of raw and preprocessed signals for all loading conditions can be found in **Supplementary Table 2**.

$$\|\boldsymbol{x_i}\| = \frac{\boldsymbol{x_i} - x_{min}}{x_{max} - x_{min}} \tag{2}$$

Here, x_{max} and x_{min} represent the maximum and minimum limits, respectively, set for all data within a specific channel.

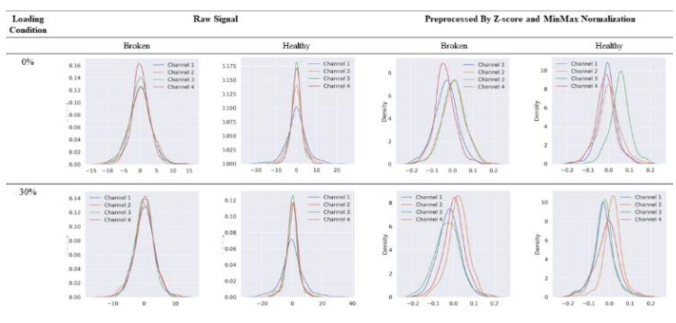

FIGURE 4. **A graphical representation of the distribution of raw and preprocessed signals at 0% and 30% loading conditions.**

This article has been accepted for publication in IEEE Access. This is the author's version which has not been fully edited and
content may change prior to final publication. Citation information: DOI 10.1109/ACCESS.2024.3412274

D. GEARFAULTNET ARCHITECTURE

Since 1D signals have only one dimension which is the signal length, the convolution is done using a $k \times 1$ kernel in 1D-CNN. If the input x_k^l of the k^{th} neuron at layer l can be defined, then the intermediate output y_k^l of that layer can be determined. x_k^l is formulated based on the output s_i^{l-1} and kernel w_i^{l-1} of the i^{th} neuron at the previous layer $l-1$. The input x_k^l can be expressed as in (3).

$$\boldsymbol{x_k^l} = b_k^l + \sum_{n=1}^{N_{l-1}} Conv1D\left(\boldsymbol{s_i^{l-1}}, w_i^{l-1}\right) \tag{3}$$

where, b_k^l represents the bias of the k^{th} neuron at layer x_k^l. The input x_k^l is passed through an activation function to generate the intermediate output y_k^l. If the activation function chosen is *tanh* (defined in (4) [51]), then the output y_k^l is calculated as in (5).

$$\boldsymbol{y_k^l} = tanh\left(\boldsymbol{x_k^l}\right) \tag{4}$$

$$tanh = \frac{1-e^{-2x}}{1+e^{-2x}} \tag{5}$$

Using (4), the final output $\hat{y}_{f\times 1}$ with the feature vector of $f \times 1$ at layer l can be formulated as in (6).

$$\boldsymbol{\hat{y}_{f\times 1}} = \sum_{k=1}^{f} \boldsymbol{y_k^l} = \sum_{k=1}^{f} tanh\left(\boldsymbol{x_k^l}\right) \tag{6}$$

MaxPooling serves to reduce the dimension of the feature map [52]. Utilizing a $k \times k$ kernel, it identifies the maximum feature within a $k \times k$ set of features with sliding increment s. The process of forward propagation of 1D-CNN with *1D-MaxPooling* is depicted in Fig. 5. If *MaxPooling* is employed to reduce the dimension of the output, then $\hat{y}$ can be formulated in (7).

$$\boldsymbol{\hat{y}_{f\times 1}} = \sum_{k=1}^{f} \boldsymbol{y_k^l} = \sum_{k=1}^{f} tanh\left(MaxPooling\left(\boldsymbol{x_k^l}\right)\right) \tag{7}$$

The input feature vector $[x_1, x_2, \dots, x_n]$ undergoes convolution with a squeezing kernel of size 3×1, as illustrated in Fig. 5. Subsequently, the convolved output is subjected to *MaxPooling* and *tanh* activation layers to obtain the final feature map for the respective feature layer.

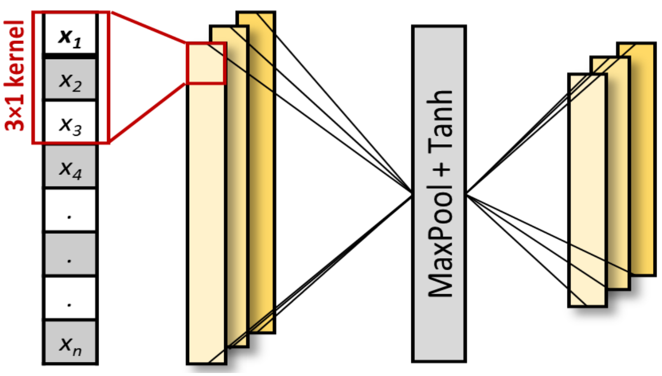

FIGURE 5. 1D Convolution followed by MaxPooling and tanh activation for an input vector of length n.

During backpropagation, the error E_p can be computed from the output of the multilayer perceptron (MLP) or densely connected layers [53] in the end. If L denotes the output layer, then for binary classification, the output vectors will be $[y_1^L, y_2^L]$ for the target vector t_p (ground truth) corresponding to an input vector p. The Soft-MMSE loss function implemented in this study has been constructed by passing the output and the target vectors through a *softmax* activation layer [54], followed by a mean squared error (MSE) layer. Consequently, the error E_p can be expressed as in (8).

$$E_p = MSE\left(softmax\left(t_p, \left[\boldsymbol{y_1^L}, \boldsymbol{y_2^L}\right]\right)\right) \tag{8}$$

Here, MSE has been formulated in (9),

$$MSE = \frac{\sum_{i=1}^{n}\left(\boldsymbol{x_i} - \boldsymbol{\hat{x}_i}\right)^2}{n} \tag{9}$$

In this case, x_i and $\hat{x}_i$ denote the ith ground truth and estimated sample, respectively. The *GearFaultNet*, introduced in this study, comprises five sequentially connected 1D-CNN blocks, as illustrated in Fig. 5. The initial layer includes a *MaxPooling* layer to downsample the input feature map. The data from the four sensors employed for the gear fault classification task resulted in the input vector having a dimension of (4×512). In the first convolutional block, the channel-wise dimension was augmented by employing additional convolutional kernels or filters, while the length of the feature map was downscaled by a *MaxPooling* layer with a *stride* of 2. The dimension of the feature map is varied while sequentially passing through the intermediate four 1D-CNN blocks having a fixed set of filters: {32, 16, 32, 24}. After the fifth 1D-CNN block, the feature map is efficiently reduced through an *Adaptive-Average-Pooling* [55] layer that makes its length to be 8. The output of the *Adaptive-Average-Pooling* layer is passed through a *Flatten* layer [56] to convert the feature map into a single dimension before transmitting it to a block consisting of densely connected MLP layers. The dense layers further process the input feature maps from the CNN layers with the assistance of densely connected neurons [53]. The final layer of the MLP block comprises two neurons, facilitating the binary classification process to discern *Broken* and *Healthy* signals and identify faults in mechanical gears based on the fine-tuned features. We use the widely used *Adam* optimizer [57] to guide the learning process of GearFaultNet and reach optimum performance with the available data. The architecture of the *GearFaultNet* is illustrated in Fig. 6. Detailed model parameters have been provided in **Supplementary Table 3**.

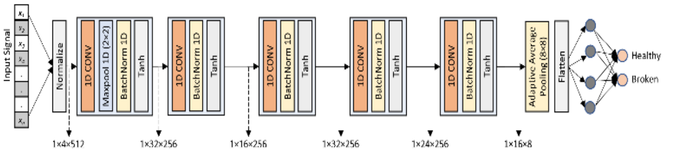

FIGURE 6. GearFaultNet architecture.

E. EXPERIMENTAL SETUP

In this research, we employ gear fault data collected under 10 distinct loading conditions and adopt a 'leave-one-out' approach to construct training and evaluation folds. By reserving data from one loading condition for testing and utilizing the rest for training and validation, we create tenfold cross-validation sets. Google ColabPro serves as the platform for conducting our experiments, utilizing a 16 GB Tesla T4 GPU and 12 GB of RAM. To optimize performance, we explore various hyperparameter tuning methods, including adjusting the batch size to optimize GPU memory usage, employing a lower learning rate for improved convergence, and increasing the number of epochs to enhance accuracy. Additionally, techniques such as epoch patience and *EpochsStoppingCriteria* [58] are employed to regulate the learning rate based on validation loss and mitigate issues of underfitting and overfitting, respectively. General hyperparameter settings utilized in the study are outlined in **TABLE I**.

TABLE I
EXPERIMENTAL CONFIGURATIONS

Training Parameters	Models
Batch size	4
Number of epochs	200
Epochs patience	10
Learning rate	0.0002
Epoch stopping criteria	30
Optimizer	Adam
Loss function	Soft-MMSE
Learning rate reduction factor	0.2

F. EVALUATION METRICS

To evaluate the gear fault classification performance of *GearFaultNet*, we employ standard evaluation metrics for classifiers such as accuracy (10), precision (11), recall or sensitivity (12), specificity (13), and F1-score (14).

$$Accuracy = \frac{TP + TN}{TP + TN + FP + FN} \tag{10}$$

$$Precision = \frac{TP}{TP + FN} \tag{11}$$

$$Recall\ or\ Sensitivity = \frac{TP}{TP + FP} \tag{12}$$

$$Speicificity = \frac{TN}{TN + FP} \tag{13}$$

$$F1 - score = \frac{2TP}{2TP + FP + FN} \equiv \frac{2 * Precision * Recall}{Precision + Recall} \tag{14}$$

Here, TP, TN, FP and FN denote true positive, true negative, false positive, and false negative, respectively. F1-score represents the harmonic mean of precision and recall, as shown in (14). We utilize both weighted and overall accuracy to present the performance of *GearFaultNet*. In addition to accuracy, other metrics are weighted based on the samples per class.

In addition to these metrics, for a comprehensive understanding of the overall performance across classes, we aggregate the test results from all 10 folds to construct a confusion matrix. This matrix illustrates the classification model's performance in terms of TP, TN, FP, and FN counts [59]. Indeed, these four counts derived from the confusion metrics were utilized to calculate higher-level evaluation metrics such as accuracy, precision, recall, F1-score, and specificity, as previously discussed. Furthermore, we depict the per-class, micro, and macro-average receiver operating characteristic (ROC) curves based on *GearFaultNet's* performance. A ROC curve illustrates the performance of a classification model across all classification thresholds, plotting two parameters: true positive rate (TPR) and false positive rate (FPR) [60]. Additionally, we present the area under the ROC curve (AUC or AUROC) for each of the four variables (per-class, micro, and macro-average) [60].

IV. RESULTS

In this section, we provide experimental outcomes of this research along with relevant discussions in detail. First, we assess the effectiveness of *GearFaultNet* in detecting gear faults by examining the aforementioned evaluation metrics. Subsequently, we juxtapose *GearFaultNet*'s performance in 1D classification with several commonly employed state-of-the-art (SOTA) models within the relevant field. Additionally, we analyze *GearFaultNet*'s performance in comparison to methodologies proposed in the existing literature.

A. GEAR FAULT DETECTION PERFORMANCE

TABLE II presents the comprehensive performance evaluation of *GearFaultNet* in detecting gear faults using accelerometer-recorded vibration data. The model achieves a weighted accuracy and an overall accuracy of 94.06%. Moreover, the weighted precision, recall, and specificity of the model are 94.11%, 94.06%, and 94.01%, respectively. The weighted F1-score of *GearFaultNet* stands at 94.05%, a crucial metric for gauging overall model performance given the dataset's uneven class distribution.

TABLE II
DETAILED PERFORMANCE OF GEARFAULTNET

Class	Accuracy		Precision	Recall	F1-score	Specificity
	Weighted	Overall				
Broken	94.06	-	95.60	92.21	93.87	95.86
Healthy	94.06	-	92.66	95.86	94.23	92.21
Overall	94.06	94.06	94.11	94.06	94.05	94.01

In **TABLE II**, we also detail the model's performance individually for each class. The precision is higher for the *Broken* class but lower for the *Healthy* class. Conversely, recall displays the opposite trend for both classes. Because of this ambiguity observed among these higher-level metrics, we calculate the confusion matrix as elaborated below

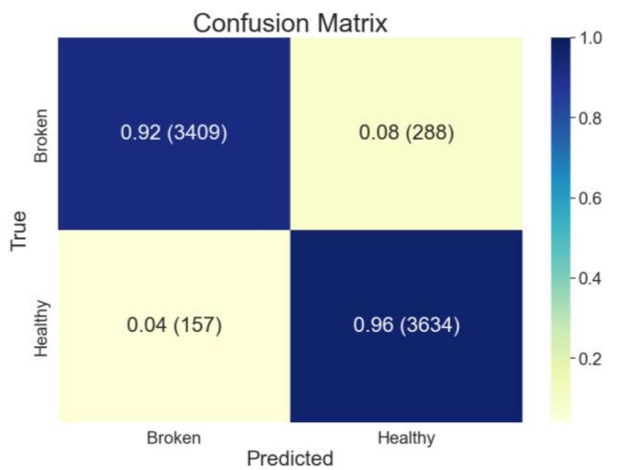

FIGURE 7. Overall confusion matrix for gear fault detection using the novel GearFaultNet.

Fig. 7 depicts the confusion matrix of the proposed

This article has been accepted for publication in IEEE Access. This is the author's version which has not been fully edited and
content may change prior to final publication. Citation information: DOI 10.1109/ACCESS.2024.3412274

GearFaultNet. Here, the *Broken* cases are designated as positive, while *Healthy* cases are regarded as negative. Across all 10 folds, there are 7,488 test samples, comprising 3,697 instances for *Broken* conditions and 3,791 instances for *Healthy* conditions. Among the 3,697 samples representing *Broken* conditions, 3,409 were correctly predicted as true positives, while 288 were incorrectly classified as false negatives. Conversely, out of the 3,791 *Healthy* samples, 3,634 were accurately predicted as true negatives. However, there were 157 instances of false positive predictions, where signals were erroneously classified as *Broken* despite being labeled as *Healthy*. Both overall and per-class metrics detailed in **TABLE II** were derived from the confusion matrix depicted in Fig. 7. Nevertheless, it is apparent from the confusion matrix that the proposed model exhibited superior performance in classifying *Healthy* instances compared to *Broken* cases.

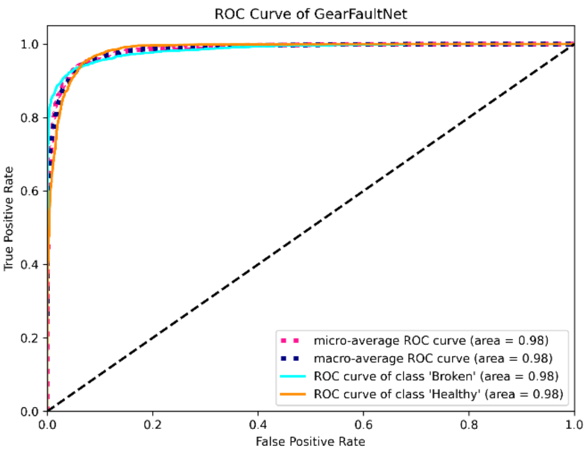

FIGURE 8. ROC curves and AUROC for GearFaultNet in terms of per-class, macro and micro measures.

On the other hand, Fig. 8 illustrates the ROC curves for each class (*Healthy* and *Broken*), as well as the macro- and micro-averages of the predictions. The x-axis of the ROC curves represents the false positive rate (FPR), while the y-axis represents the true positive rate (TPR). The ROC curves plotted in Fig. 8 reveal that, for all macro- and micro-averages, as well as the individual classes, the TPR almost reaches 1 within the FPR range of 0.1 to 0.2. It is noteworthy that both *Broken* and *Healthy* classes, as well as the micro- and macro-averages, exhibit the same AUC or AUROC of 0.98 or 98%. These observations further confirm *GearFaultNet's* capability to distinguish between *Broken* and *Healthy* cases, beyond the traditional classification metrics. The training curve, loss curve, and fold-wise accuracy provide additional insights into *GearFaultNet's* fold-wise performance, all of which have been outlined in **Supplementary Table 1**.

B. COMPARISON WITH SOTA MODELS

In this ablation study, we trained and evaluated two cutting-edge 1D-classification models, namely ResNet18 [61] and Self-ResNet18, while adhering to the experimental configurations outlined in **TABLE I**, to compare their performance with that of *GearFaultNet*. The 1D-ResNet18 model utilized in this investigation is based on the ResNet18 architecture, a pioneering deep learning model introduced by He et al. [61] in 2015 for 2D image classification. ResNet models have been widely adopted across various 1D and 2D domains due to their efficacy and lightweight nature. We developed Self-ResNet18, a variant of the original architecture known as an operational neural network (ONN) [62], by replacing its conventional CNN layers with self-ONN layers [63]. The outcomes of this ablation study are presented in **TABLE III**.

TABLE III
GEARFAULTNET AGAINST SOTA MODELS

Models	Accuracy	Precision	Sensitivity	F1-score	Specificity
ResNet18 [61]	77.74	78.10	77.74	77.64	77.58
Self-ResNet18	92.74	93.20	92.74	92.71	92.60
GearFaultNet	94.06	94.11	94.06	94.05	94.01

From **TABLE III**, it is evident that *GearFaultNet* attained the highest accuracy of 94.06%, closely trailed by Self-ResNet18 at 92.74%, and ResNet18 at 77.74%. Precision, sensitivity, and F1-score metrics likewise exhibit the consistent superiority of *GearFaultNet* over the two state-of-the-art (SOTA) models. Furthermore, *GearFaultNet* displayed well-rounded performance across all metrics, showcasing high precision, sensitivity, and specificity, which indicates its efficacy in accurately detecting gear faults.

C. COMPARISON WITH EXISTING STUDIES

TABLE IV presents the performance of *GearFaultNet* compared to studies in the current literature. While our proposed method's results did not surpass those reported by [2], the preprocessing approach fundamentally differed between the two studies. For instance, before the 10-fold split, the authors in [2] employed sample shuffling, which could potentially lead to data leakage in the train and test sets. Conversely, in this study, we adopted the more challenging "leave-one-out" strategy for train-test splitting, affirming the robustness of the process. Additionally, *GearFaultNet* outperformed the performance reported in the literature by [3]. This enhancement in *GearFaultNet's* performance highlights its effectiveness in distinguishing between *Broken* and *Healthy* signals compared to the currently best-performing studies.

TABLE IV
GEARFAULTNET AGAINST EXISTING STUDIES

Study	Method	Accuracy
[2]	NLMS Error (Adaptive filter) + SVM	100%
	EMD-IMF 1 + SVM	100%
	Plain Method + SVM	100%
[3]	Sigmoid-PSO + Hybrid LSTM	87.50%
	ReLU-Cuckoo + Hybrid LSTM	87.50%
Current	**1D Deep Classifier (GearFaultNet)**	94.06%

V. CONCLUSION

Detecting gearbox faults in rotating machinery is crucial for averting catastrophic machine breakdowns. Vibration signals are commonly employed in fault diagnosis across various loading conditions. This study introduces a novel 1D-CNN model, *GearFaultNet*, after incorporating standard preprocessing steps like z-score and min-max normalization during data preparation. The adoption of such normalization methods reduces the computational time compared to complex preprocessing techniques proposed in prior studies. The proposed *GearFaultNet* demonstrates significant performance enhancement with its expedited preprocessing technique and lightweight deep learning model. *GearFaultNet* achieves an overall accuracy, precision, and specificity of 94.06%, 94.11%, and 94.01%, respectively, in classifying *Broken* and *Healthy* signals. These classification results notably surpass those reported in contemporary literature for gearbox fault detection. Such a precise model can facilitate the differentiation between *Healthy* and *Broken* vibration signals in industrial sectors for real-time monitoring, and its scope can also be extended to similar domains. Future endeavors could focus on seeking even more accurate and lightweight models to further improve performance while maintaining reliability and portability. Furthermore, compiling a more diverse dataset with additional data from various sensors could enable early detection of *Broken* conditions from real-time sensor data.

DATA AVAILABILITY

The data that support the findings of this study are available in [35]. Pre-processed data will be shared upon request.

FUNDING

This research received no external funding. The open access publication of this article is supported by Qatar National Library.

INFORMED CONSENT STATEMENT

Not applicable

DECLARATION OF COMPETING INTEREST

The authors declare that they have no conflict of interest.

REFERENCES

[1] Y. Peng, W. Qiao, F. Cheng, and L. Qu, "Wind Turbine Drivetrain Gearbox Fault Diagnosis Using Information Fusion on Vibration and Current Signals," in IEEE Transactions on Instrumentation and Measurement, vol. 70, pp. 1-11, 2021, Art no. 3518011, doi: 10.1109/TIM.2021.3083891.

[2] J. Vrba, M. Cejnek, J. Steinbach, and Z. Krbcova, "A machine learning approach for gearbox system fault diagnosis," Entropy (Basel), vol. 23, no. 9, p. 1130, 2021, doi: 10.3390/e23091130.

[3] G. Krishna Durbhaka, B. Selvaraj, M. Mittal, T. Saba, A. Rehman, and L. Mohan Goyal, “Swarm-LSTM: Condition monitoring of gearbox fault diagnosis based on hybrid LSTM deep neural network optimized by swarm intelligence algorithms,” Comput. Mater. Contin., vol. 66, no. 2, pp. 2041–2059, 2021, doi: 10.32604/cmc.2020.013131.

[4] J. Yu, X. Zhou, L. Lu, and Z. Zhao, "Multiscale Dynamic Fusion Global Sparse Network for Gearbox Fault Diagnosis," in IEEE Transactions on Instrumentation and Measurement, vol. 70, pp. 1-11, 2021, Art no. 3516111, doi: 10.1109/TIM.2021.3076855.

[5] L. Lu, Y. He, Y. Ruan, and W. Yuan, "Wind Turbine Planetary Gearbox Condition Monitoring Method Based on Wireless Sensor and Deep Learning Approach," in IEEE Transactions on Instrumentation and Measurement, vol. 70, pp. 1-16, 2021, Art no. 3503016, doi: 10.1109/TIM.2020.3028402.

[6] G. K. Balakrishnan et al., "A review of infrared thermography for condition-based monitoring in electrical energy: Applications and recommendations," Energies, vol. 15, no. 16, p. 6000, 2022, doi: 10.3390/en15166000.

[7] H. Malik, A. Iqbal, and A. K. Yadav, Soft computing in condition monitoring and diagnostics of electrical and mechanical systems. Springer, 2020.

[8] S. Muller, M. Deicke and R. W. De Doncker, "Doubly fed induction generator systems for wind turbines," in IEEE Industry Applications Magazine, vol. 8, no. 3, pp. 26-33, May-June 2002, doi: 10.1109/2943.999610.

[9] Y. Wang, S. Yang, and R. V. Sánchez, "Gearbox Fault Diagnosis Based on a Novel Hybrid Feature Reduction Method," in IEEE Access, vol. 6, pp. 75813-75823, 2018, doi: 10.1109/ACCESS.2018.2882801.

[10] H. Haes Alhelou, M. E. Hamedani-Golshan, T. C. Njenda, and P. Siano, "A survey on power system blackout and cascading events: Research motivations and challenges," Energies, vol. 12, no. 4, p. 682, 2019.

[11] H. Malik, Y. Pandya, A. Parashar, and R. Sharma, “Feature extraction using EMD and classifier through artificial neural networks for gearbox fault diagnosis,” in Advances in Intelligent Systems and Computing, Singapore: Springer Singapore, 2019, pp. 309–317, doi: 10.1007/978-981-13-1822-1_28.

[12] S. A. Hossain, M. A. Rahman, A. Chakrabarty, M. A. Rashid, A. Kuwana, and H. Kobayashi, "Emotional State Classification from MUSIC-Based Features of Multichannel EEG Signals," Bioengineering, vol. 10, no. 1, p. 99, 2023, doi: 10.3390/bioengineering10010099.

[13] M. Sakib Abrar Hossain, M. Asadur Rahman and A. Chakrabarty, "MUSIC Model based Neural Information Processing for Emotion Recognition from Multichannel EEG Signal," 2021 8th International Conference on Signal Processing and Integrated Networks (SPIN), Noida, India, 2021, pp. 955-960, doi: 10.1109/SPIN52536.2021.9565974.

[14] S. Rajendran, W. Meert, D. Giustiniano, V. Lenders and S. Pollin, "Deep Learning Models for Wireless Signal Classification With Distributed Low-Cost Spectrum Sensors," in IEEE Transactions on Cognitive Communications and Networking, vol. 4, no. 3, pp. 433-445, Sept. 2018, doi: 10.1109/TCCN.2018.2835460.

[15] Z. Chen, C. Li, and R.-V. Sanchez, "Gearbox fault identification and classification with convolutional neural networks," Shock and Vibration, vol. 2015, 2015, doi: 10.1155/2015/390134.

[16] C. Lu, Z. Wang, and B. Zhou, "Intelligent fault diagnosis of rolling bearing using hierarchical convolutional network-based health state classification," Advanced Engineering Informatics, vol. 32, pp. 139-151, 2017, doi: 10.1016/j.aei.2017.02.005.

[17] V. T. Tran and B.-S. Yang, “An intelligent condition-based maintenance platform for rotating machinery,” Expert Syst. Appl., vol. 39, no. 3, pp. 2977–2988, 2012, doi: 10.1016/j.eswa.2011.08.159.

[18] K. Kumar, K. Rao, K. Krishna, and B. Theja, "Neural network based vibration analysis with novelty in data detection for a large steam turbine," Shock and Vibration, vol. 19, no. 1, pp. 25-35, 2012, doi: 10.3233/SAV-2012-0614.

[19] L.-l. Jiang, H.-k. Yin, X.-j. Li, and S.-w. Tang, "Fault diagnosis of rotating machinery based on multisensor information fusion using SVM and time-domain features," Shock and Vibration, vol. 2014, 2014, doi: 10.1155/2014/418178.

[20] X. Liu, Q. Zhou, J. Zhao, H. Shen, and X. Xiong, "Fault diagnosis of rotating machinery under noisy environment conditions based on a 1-D convolutional autoencoder and 1-D convolutional neural network," Sensors, vol. 19, no. 4, p. 972, 2019, doi: 10.3390/s19040972.

[21] P. Cao, S. Zhang, and J. Tang, "Preprocessing-Free Gear Fault Diagnosis Using Small Datasets With Deep Convolutional Neural Network-Based Transfer Learning," in IEEE Access, vol. 6, pp. 26241-26253, 2018, doi: 10.1109/ACCESS.2018.2837621.

[22] H. S. Dhiman, D. Deb, S. Muyeen, and I. Kamwa, "Wind turbine gearbox anomaly detection based on adaptive threshold and twin support vector machines," IEEE Transactions on Energy Conversion, vol. 36, no. 4, pp. 3462-3469, 2021, doi: 10.1109/TEC.2021.3075897.

[23] M. Azamfar, J. Singh, X. Li, and J. Lee, "Cross-domain gearbox diagnostics under variable working conditions with deep convolutional transfer learning," Journal of Vibration and Control, vol. 27, no. 7-8, pp. 854-864, 2021, doi: 10.1177/1077546320933793.

[24] Z. Chen, S. Deng, X. Chen, C. Li, R.-V. Sanchez, and H. Qin, "Deep neural networks-based rolling bearing fault diagnosis," Microelectronics Reliability, vol. 75, pp. 327-333, 2017, doi: 10.1016/j.microrel.2017.03.006.

[25] G. Liu, H. Bao, and B. Han, "A stacked autoencoder-based deep neural network for achieving gearbox fault diagnosis," Mathematical Problems in Engineering, vol. 2018, pp. 1-10, 2018, doi: 10.1155/2018/5105709.

[26] Y. Yao, S. Zhang, S. Yang, and G. Gui, "Learning attention representation with a multi-scale CNN for gear fault diagnosis under different working conditions," Sensors, vol. 20, no. 4, p. 1233, 2020, doi: 10.3390/s20041233.

[27] B. Merainani, C. Rahmoune, D. Benazzouz, and B. Ould-Bouamama, "A novel gearbox fault feature extraction and classification using

Hilbert empirical wavelet transform, singular value decomposition, and SOM neural network," Journal of Vibration and Control, vol. 24, no. 12, pp. 2512-2531, 2018, doi: 10.1177/1077546316688991.
[28] C. Li, R.-V. Sanchez, G. Zurita, M. Cerrada, D. Cabrera, and R. E. Vásquez, "Gearbox fault diagnosis based on deep random forest fusion of acoustic and vibratory signals," Mechanical Systems and Signal Processing, vol. 76, pp. 283-293, 2016, doi: 10.1016/j.ymssp.2016.02.007.
[29] P. Wang, R. Yan, and R. X. Gao, "Virtualization and deep recognition for system fault classification," Journal of Manufacturing Systems, vol. 44, pp. 310-316, 2017, doi: 10.1016/j.jmsy.2017.04.012.
[30] Z. Ye and J. Yu, "AKRNet: A novel convolutional neural network with attentive kernel residual learning for feature learning of gearbox vibration signals," Neurocomputing, vol. 447, pp. 23-37, 2021, doi: 10.1016/j.neucom.2021.02.055.
[31] S. -N. Chen, F. Liu, C. -X. Gao and J. Li, "Gearbox Fault Diagnosis Classification with Empirical Mode Decomposition Based on Improved Long Short-Term Memory," 2021 IEEE 6th International Conference on Cloud Computing and Big Data Analytics (ICCCBDA), Chengdu, China, 2021, pp. 568-575, doi: 10.1109/ICCCBDA51879.2021.9442505.
[32] M. Zhao, M. Kang, B. Tang, and M. Pecht, "Deep residual networks with dynamically weighted wavelet coefficients for fault diagnosis of planetary gearboxes," IEEE Transactions on Industrial Electronics, vol. 65, no. 5, pp. 4290-4300, 2017, doi: 10.1109/TIE.2017.2762639.
[33] H. Wang, J. Xu, C. Sun, R. Yan, and X. Chen, "Intelligent fault diagnosis for planetary gearbox using time-frequency representation and deep reinforcement learning," IEEE/ASME Transactions on Mechatronics, vol. 27, no. 2, pp. 985-998, 2021, doi: 10.1109/TMECH.2021.3076775.
[34] J. He, S. Yang, and C. Gan, "Unsupervised fault diagnosis of a gear transmission chain using a deep belief network," Sensors, vol. 17, no. 7, p. 1564, 2017, doi: 10.3390/s17071564.
[35] data.world. "Gearbox fault diagnosis dataset." https://data.world/gearbox/gear-box-fault-diagnosis-data-set. (accessed Feb 12, 2024).
[36] Machinelearningmastery.com. [Online]. Available: https://machinelearningmastery.com/data-leakage-machine-learning/. (accessed May 11, 2024).
[37] SpectraQuest.Inc. "SpectraQuest's Gearbox Prognostics Simulator (GPS)." https://spectraquest.com/prognostics/details/gps/ (accessed Feb 12, 2024)
[38] S. Mahmud et al., "A shallow U-net architecture for reliably predicting blood pressure (BP) from photoplethysmogram (PPG) and electrocardiogram (ECG) signals," Sensors (Basel), vol. 22, no. 3, p. 919, 2022, doi: 10.3390/s22030919.
[39] N. Ibtehaz et al., "PPG2ABP: Translating photoplethysmogram (PPG) signals to arterial blood pressure (ABP) waveforms," Bioengineering, vol. 9, no. 11, p. 692, 2022, doi: 10.3390/bioengineering9110692.
[40] S. Mahmud et al., "NABNet: A nested attention-guided BICONVLSTM network for a robust prediction of blood pressure components from reconstructed arterial blood pressure waveforms using PPG and ECG signals," Biomedical Signal Processing and Control, vol. 79, p. 104247, 2023, doi: 10.1016/j.bspc.2022.104247.
[41] M. G. Ragab, S. J. Abdulkadir, N. Aziz, H. Alhussian, A. Bala, and A. Alqushaibi, "An ensemble one-dimensional convolutional neural network with Bayesian optimization for environmental sound classification," Applied Sciences, vol. 11, no. 10, p. 4660, 2021, doi: 10.3390/app11104660.
[42] N. R. Nurwulan and B. C. Jiang, "Window selection impact in human activity recognition," International Journal of Innovative Technology and Interdisciplinary Sciences, vol. 3, no. 1, pp. 381-394, 2020, doi: 10.15157/IJITIS.2020.3.1.381-394.
[43] N. N. Nisha et al., "A Deep Learning Framework for the Detection of Abnormality in Cerebral Blood Flow Velocity Using Transcranial Doppler Ultrasound," Diagnostics, vol. 13, no. 12, p. 2000, 2023, doi: 10.3390/diagnostics13122000.
[44] K. K. Podder et al., "Deep learning-based middle cerebral artery blood flow abnormality detection using flow velocity waveform derived from transcranial Doppler ultrasound," Biomedical Signal Processing and Control, vol. 85, p. 104882, 2023, doi: 10.1016/j.bspc.2023.104882.
[45] S. Mahmud et al., "Wearable wrist to finger photoplethysmogram translation through restoration using super operational neural networks based 1D-CycleGAN for enhancing cardiovascular monitoring," Expert Syst. Appl., vol. 246, no. 123167, p. 123167, 2024, doi: 10.1016/j.eswa.2024.123167.
[46] S. Mahmud, M. S. Hossain, M. E. Chowdhury, and M. B. Reaz, "MLMRS-net: Electroencephalography (EEG) motion artifacts removal using a multi-layer multi-resolution spatially pooled 1D signal reconstruction network," Neural Computing and Applications, vol. 35, no. 11, pp. 8371–8388, 2022, doi: 10.1007/s00521-022-08111-6.
[47] S. Mahmud et al., "Restoration of motion-corrupted EEG signals using attention-guided operational CycleGAN," Eng. Appl. Artif. Intell., vol. 128, no. 107514, p. 107514, 2024, doi: 10.1016/j.engappai.2023.107514.
[48] M. S. Hossain et al., "MultiResUNet3+: A full-scale connected multi-residual UNet model to denoise electrooculogram and electromyogram artifacts from corrupted electroencephalogram signals," Bioengineering (Basel), vol. 10, no. 5, p. 579, 2023, doi: 10.3390/bioengineering10050579.
[49] M. I. Tapotee, P. Saha, S. Mahmud, A. Alqahtani, and M. E. H. Chowdhury, "M2ECG: Wearable mechanocardiograms to electrocardiogram estimation using deep learning," IEEE Access, vol. 12, pp. 12963–12975, 2024, doi: 10.1109/ACCESS.2024.3353463.
[50] M. Z. Al-Faiz, A. A. Ibrahim, and S. M. Hadi, "The effect of Z-Score standardization (normalization) on binary input due to the speed of learning in the back-propagation neural network," Iraqi Journal of Information and Communication Technology, vol. 1, no. 3, pp. 42-48, 2018, doi: 10.31987/ijict.1.3.41.
[51] "Tanh — PyTorch 2.3 documentation," Pytorch.org. [Online]. Available: https://pytorch.org/docs/stable/generated/torch.nn.Tanh.html. (accessed May 08, 2024).
[52] "MaxPool1d — PyTorch 2.3 documentation," Pytorch.org. [Online]. Available: https://pytorch.org/docs/stable/generated/torch.nn.MaxPool1d.html. (accessed May 08, 2024).
[53] S. Abirami and P. Chitra, "Energy-efficient edge-based real-time healthcare support system," in Advances in Computers, Elsevier, 2020, pp. 339–368, doi: 10.1016/bs.adcom.2019.09.007.
[54] "Softmax — PyTorch 2.3 documentation," Pytorch.org. [Online]. Available: https://pytorch.org/docs/stable/generated/torch.nn.Softmax.html. (accessed May 08, 2024).
[55] "AdaptiveAvgPool1d — PyTorch 2.3 documentation," Pytorch.org. [Online]. Available: https://pytorch.org/docs/stable/generated/torch.nn.AdaptiveAvgPool1d.html. (accessed May 08, 2024).
[56] "torch.flatten — PyTorch 2.3 documentation," Pytorch.org. [Online]. Available: https://pytorch.org/docs/stable/generated/torch.flatten.html. (accessed May 09, 2024).
[57] D. P. Kingma and J. Ba, "Adam: A method for stochastic optimization," arXiv [cs.LG], 2014, doi: 10.48550/arXiv.1412.6980.
[58] "Early Stopping — PyTorch Lightning 2.2.3 documentation," Lightning.ai. [Online]. Available: https://lightning.ai/docs/pytorch/stable/common/early_stopping.html. (accessed May 10, 2024).
[59] S. Mahmud, T. O. Abbas, A. Mushtak, J. Prithula, and M. E. H. Chowdhury, "Kidney cancer diagnosis and surgery selection by machine learning from CT scans combined with clinical metadata," Cancers (Basel), vol. 15, no. 12, p. 3189, 2023, doi: 10.3390/cancers15123189.
[60] "Classification: ROC curve and AUC," Google for Developers. [Online]. Available: https://developers.google.com/machine-learning/crash-course/classification/roc-and-auc. (accessed May 10, 2024).
[61] K. He, X. Zhang, S. Ren and J. Sun, "Deep Residual Learning for Image Recognition," 2016 IEEE Conference on Computer Vision and Pattern Recognition (CVPR), Las Vegas, NV, USA, 2016, pp. 770-778, doi: 10.1109/CVPR.2016.90.
[62] S. Kiranyaz, T. Ince, A. Iosifidis and M. Gabbouj, "Operational neural networks", Neural Computing and Applications, vol. 32, no. 11, pp. 6645-6668, 2020, doi: 10.1007/s00521-020-04780-3.
[63] S. Kiranyaz, J. Malik, H. B. Abdallah, T. Ince, A. Iosifidis, M. Gabbouj "Self-organized Operational Neural Networks with Generative Neurons", Neural Networks (Elsevier), pp. 140:294-308, Aug. 2021, doi: 10.1016/j.neunet.2021.02.028.

This article has been accepted for publication in IEEE Access. This is the author's version which has not been fully edited and content may change prior to final publication. Citation information: DOI 10.1109/ACCESS.2024.3412274

AUTHOR BIOGRAPHY

Proma Dutta is a distinguished researcher currently pursuing her doctoral studies in Interdisciplinary Engineering at Kennesaw State University. Her primary research interests encompass the fields of Intelligent Transportation Systems, Transportation Data Analytics, Artificial Intelligence, and Machine Learning. Leveraging her academic foundation, she obtained her undergraduate degree in Electrical and Electronic Engineering from Chittagong University of Engineering and Technology, Bangladesh. Proma's academic trajectory reflects a seamless integration of her background in Electrical and Electronic Engineering into the domain of Transportation Engineering research. Her dedicated focus on the interdisciplinary intersection of engineering and technology underscores her commitment to advancing the field of Artificial Intelligence and Intelligent Transportation Systems.

Kanchon Kanti Podder is a passionate researcher in the field of intelligent robotic systems, driven by the intersection of machine learning and deep learning. His current PhD research at Kennesaw State University explores how robots can autonomously acquire manipulation skills through reinforcement learning algorithms. Podder began his academic journey with a Bachelor's degree in Electrical & Electronic Engineering from Chittagong University of Engineering & Technology, Bangladesh, and further honed his technical expertise by earning a Master's degree in Biomedical Physics and Technology from the University of Dhaka, Bangladesh. His research interests extend beyond robotics, encompassing areas like gesture recognition and silent speech recognition, which he believes can benefit from responsible and innovative use of machine learning and deep learning. He aims to contribute to these exciting advancements through his research.

Md. Shaheenur Islam Sumon, a graduate student in biomedical engineering, currently works as a Research Assistant at the Qatar University Machine Learning Group.

Muhammad E. H. Chowdhury (Senior Member, IEEE) received a Ph.D. degree from the University of Nottingham, U.K., in 2014. He worked as a Postdoctoral Research Fellow and a Hermes Fellow at the Sir Peter Mansfield Imaging Centre, University of Nottingham. He is currently working as an Assistant Professor with the Department of Electrical Engineering, at Qatar University. He has four patents and published more than 200 peer-reviewed journal articles, conference papers, and four book chapters. His current research interests include biomedical instrumentation, signal processing, wearable sensors, medical image analysis, machine learning, embedded systems design, and simultaneous EEG/fMRI. He is currently running several NPRP, UREP, and HSREP grants from QNRF and internal grants from Qatar University, and is involved in MRC grants. He has been involved in EPSRC, ISIF, and EPSRC-ACC grants along with different national and international projects. He has worked as a Consultant for the project entitled “Driver Distraction Management Using Sensor Data Cloud (2013–14, Information Society Innovation Fund (ISIF) Asia).” He received the ISIF Asia Community Choice Award 2013 for a project entitled “Design and Development of Precision Agriculture Information System for Bangladesh.” He has recently won the “COVID-19 Dataset Award” and the “National AI Competition Awards” for his contribution to the fight against COVID-19. He is serving as an Associate Editor for IEEE Access, a Topic Editor, and a Review Editor for Frontiers in Neuroscience.

Amith Khandakar (Senior Member, IEEE) graduated as the Valedictorian from North South University. He received a B.Sc. degree in electronics and telecommunication engineering from North South University, Bangladesh, and a master’s degree in computing (networking concentration) from Qatar University, in 2014. He is currently the General Secretary of the IEEE Qatar Section and also the Qatar University IEEE Student Branch Coordinator and an Adviser (Faculty). He is also a certified Project Management Professional and the Cisco Certified Network Administrator. He was a Teaching Assistant and a Laboratory Instructor for two years for courses, such as mobile and wireless communication systems, the principle of digital communications, introduction to Communication, calculus and Analytical Geometry, and Verilog HDL: modeling, simulation, and Synthesis. Simultaneously, he was a Laboratory Instructor for the following courses: programming course ‘‘C,’’ Verilog HDL, and general physics course. He has been with Qatar University, since 2010. After graduation, he was a consultant in a reputed insurance company in Qatar and in a private company that is a sub-contractor to the National Telecom Service Provider in Qatar. He was a recipient of the President Gold Medal.

Nasser Al-Emadi (Senior Member, IEEE) received the B.Sc. and M.Sc. degrees in electrical engineering from Western Michigan University, Kalamazoo, MI, USA, in 1989 and 1994, respectively, and the Ph.D. degree in power systems from Michigan State University, East Lansing, MI, USA, in 2000. He is currently the Assistant Vice President of Faculty Affairs at Qatar University, Doha, Qatar, and an Associate Professor at the Department of Electrical Engineering, Qatar University. He has wide experience in electric power systems, control, protection, and sensor interfacing, control of multiphase motor drives, and renewable energy sources, and the integration of smart grids. He is a Founding Member of the Qatar Society of Engineers and a member of the Advisory Board of the IEEE Qatar Section

Moajjem Hossain Chowdhury received a B.Sc. degree in electrical and electronics engineering from North South University, Bangladesh. He is currently working as a Research Assistant at Qatar University. His current research interests include biomedical signal processing, machine learning, and data science. He placed in the top 30 in Bangladesh Physics Olympiad 2014.

M. Murugappan (Senior Member, IEEE) received a Ph.D. degree in mechatronic engineering from Universiti Malaysia Perlis, Malaysia, in 2010. Since February 2016, he has been an Associate Professor with the Department of Electronics and Communication Engineering, Kuwait College of Science and Technology (KCST) (Private University), Kuwait. He has gained more than ten years of post-Ph.D. teaching and research experience from different countries (India, Malaysia, and Kuwait). Recently, he has been included in the top 2% of scientists in the world in experimental psychology and artificial intelligence by Stanford University researchers. He has published more than 130 research articles in peer-reviewed conference proceedings/journals/book chapters. He has a maximum citation of 6972, an H-index of 42, and an i10 index of 88 (Ref: Google Scholar citations). He secured nearly $2.5 Million in research grants from the Government of Malaysia, Malaysia, and the Kuwait Foundation for Advancement of Sciences (KFAS), Kuwait for continuing his research works and successfully guided 14 postgraduate students (9 Ph.D. and 5 M.Sc.). His research interests include affective computing, the Internet of Things (IoT), the Internet of Medical Things (IoMT), cognitive neuroscience, brain-computer interface, neuromarketing, medical image processing, machine learning, and artificial intelligence. He has received Technology (KCST) (Private University), Kuwait. He has gained more than ten years of post-Ph.D. teaching and research experience from different countries (India, Malaysia, and Kuwait). Recently, he has been included in the top 2% of scientists in the world in experimental psychology and artificial intelligence by Stanford University researchers. He has published more than 130 research articles in peer-reviewed conference proceedings/journals/book chapters. He has got a maximum citation of 6972 and the H-index of 42 and i10 index of 88 (Ref: Google Scholar citations). He secured nearly $2.5 Million in research grants from the Government of Malaysia, Malaysia, and the Kuwait Foundation for Advancement of Sciences (KFAS), Kuwait for continuing his research works and successfully guided 14 postgraduate students (9 Ph.D. and 5 M.Sc.). His research interests include affective computing, the Internet of Things (IoT), the Internet of Medical Things (IoMT), cognitive neuroscience, brain-computer interface, neuromarketing, medical image processing, machine learning, and artificial intelligence. He has received several research awards, medals, and certificates for excellent publications and research products. He is also serving as a Chair for Educational Activities in the IEEE Kuwait Section. He is serving as an Editorial Board Member for PLoS ONE, Journal of Medical Imaging and Health Informatics, and International Journal of Cognitive Informatics.

Mohamed Arselene Ayari is an Associate Professor affiliated with the College of Engineering at Qatar University in Doha, Qatar. His research interests include Machine learning, deep learning, and computer vision. He has published more than 70 research articles in peer-reviewed conference proceedings/journals/book chapters. He has got a maximum citation of 1227 and the H-index of 19 and i10 index of 25 (Ref: Google Scholar citations).

Sakib Mahmud earned his Bachelor of Science (BSc.) degree in Electrical Engineering with Honors from Qatar University (QU) in June 2020, followed by the completion of his Master of Science (MSc.) degree in Electrical Engineering from the same department in May 2023. Currently, he serves as a research associate at Qatar University. With a prolific academic output, he has contributed 41 peer-reviewed journal articles to esteemed journals, comprising 33 in Q1 and 8 in Q2 categories, in addition to 3 conference papers. His expertise encompasses diverse domains, including machine learning, biomedical instrumentation, signal processing, image processing, bioinformatics, and 3D modeling.

S. M. Muyeen (Fellow, IEEE) received the B.Sc. Eng. degree in electrical and electronic engineering from the Rajshahi University of Engineering and Technology (RUET, formerly known as the Rajshahi Institute of Technology), Bangladesh, in 2000, and the M.Eng. and Ph.D. degrees in electrical and electronic engineering from the Kitami Institute of Technology, Japan, in 2005 and 2008, respectively. Currently, he is a Full Professor at the Electrical Engineering Department, at Qatar University. He has been a keynote speaker and an invited speaker at many international conferences, workshops, and universities. He has published more than 250 papers in different journals and international conferences. He has published seven books as the author or editor. His research interests include power system stability and control, electrical machines, FACTS, energy storage systems (ESSs), renewable energy, and HVdc systems. He is a fellow of Engineers Australia. He is serving as an Editor/Associate Editor for many prestigious journals from IEEE, IET, and other publishers, including IEEE Transactions on Energy Conversion, IEEE Power Engineering Letters, IET Renewable Power Generation, and IET Generation, Transmission and Distribution.